Reactions of $[NEt_4][10\text{-}endo\text{-}\{Au(PPh_3)\}\text{-}7,8\text{-}R'_2\text{-}nido\text{-}7,8\text{-}C_2B_9H_9]$ (R′ = Me or H): Synthesis of Platinum–Gold Complexes

John C. Jeffery,[1a] Paul A. Jelliss,[1a] and F. Gordon A. Stone*,[1b]

School of Chemistry, The University, Bristol BS8 1TS, U.K., and Department of Chemistry, Baylor University, Waco, Texas 76798-7348

Received April 15, 1993

Reactions between the reagents $[NEt_4][10\text{-}endo\text{-}\{Au(PPh_3)\}\text{-}7,8\text{-}R'_2\text{-}nido\text{-}7,8\text{-}C_2B_9H_9]$ (**1**, R′ = Me or H) and the compounds $[PtCl(R)L_2]$ (R = H, L = PEt_3; R = Me, L = PMe_2Ph) in CH_2Cl_2 at room temperature afford the platinum–gold complexes $[10\text{-}exo\text{-}\{Pt(R)L_2\}\text{-}10\text{-}(\mu\text{-}H)\text{-}10\text{-}endo\text{-}\{Au(PPh_3)\}\text{-}7,8\text{-}R'_2\text{-}nido\text{-}7,8\text{-}C_2B_9H_8]$ (**2**, R = H or Me, R′ = H or Me, L = PEt_3 or PMe_2Ph). The crystal structure of **2a** (R = H, R′ = Me, L = PEt_3) has been determined by X-ray diffraction. The $7,8\text{-}Me_2\text{-}nido\text{-}7,8\text{-}C_2B_9H_9$ cage is bonded to both metal atoms *via* the open pentagonal CCBBB face. The $Au(PPh_3)$ group is *endo*-attached to the three boron atoms in this face [Au–B = 2.57(2), 2.22(2), and 2.58(2) Å] with the shortest connectivity to the boron which is in the β site with respect to the two carbons [P–Au–B_β = 172.0(5)°]. The platinum atom also is linked to the carborane cage *via* B_β, through a three-center two-electron exopolyhedral B_β–H→Pt bond [Pt–B = 2.63(2) Å]. The two PEt_3 groups ligate the platinum in a transoid manner [P–Pt–P = 163.6(2)°; Pt–P average 2.298 Å], while the terminal hydrido ligand is transoid to the B_β–H bond. The Pt–Au separation is 3.000(1) Å. The structure may be regarded as zwitterionic, comprising a cationic $[PtH(PEt_3)_2]^+$ fragment linked to the anion $[10\text{-}endo\text{-}\{Au(PPh_3)\}\text{-}7,8\text{-}Me_2\text{-}nido\text{-}7,8\text{-}C_2B_9H_9]^-$ by the B_β–H→Pt bond and further anchored by the Pt–Au contact. The NMR data (^1H, $^{13}C\{^1H\}$, $^{31}P\{^1H\}$, and $^{11}B\{^1H\}$) for the new compounds are reported and discussed in the context of their structures and those of related complexes.

Introduction

The isolobal mapping of the anions $[10\text{-}endo\text{-}\{Au(PPh_3)\}\text{-}7,8\text{-}R'_2\text{-}nido\text{-}7,8\text{-}C_2B_9H_9]^-$ and $[10\text{-}endo\text{-}H\text{-}7,8\text{-}R'_2\text{-}nido\text{-}7,8\text{-}C_2B_9H_9]^-$ (R′ = Me or H) suggested using salts of the former as reagents to prepare complexes in which gold is bonded to transition elements. We have recently demonstrated use of this preparative procedure in the synthesis of several gold–rhodium and –iridium complexes.[2] Moreover, several of the products have unusual molecular structures as a consequence of the nonspectator role played by the carborane cage ligands.

Herein we report the synthesis of platinum–gold complexes from reactions between the salts $[NEt_4][10\text{-}endo\text{-}\{Au(PPh_3)\}\text{-}7,8\text{-}R'_2\text{-}nido\text{-}7,8\text{-}C_2B_9H_9]$ (R′ = Me (**1a**), H (**1b**)) and the compounds $[PtCl(H)(PEt_3)_2]$ and $[PtCl(Me)(PMe_2Ph)_2]$.

Results and Discussion

Reactions between mixtures of either of the compounds **1** and $\{PtCl(H)(PEt_3)_2\}$ in CH_2Cl_2 at room temperature afford the complexes $[10\text{-}exo\text{-}\{Pt(H)(PEt_3)_2\}\text{-}10\text{-}(\mu\text{-}H)\text{-}10\text{-}endo\text{-}\{Au(PPh_3)\}\text{-}7,8\text{-}R'_2\text{-}nido\text{-}7,8\text{-}C_2B_9H_8]$ (R′ = Me (**2a**), H (**2b**)), isolated by column chromatography and crystallization. In a similar manner, treatment of the reagents **1** with $[PtCl(Me)(PMe_2Ph)_2]$ yields the compounds $[10\text{-}exo\text{-}\{Pt(Me)(PMe_2Ph)_2\}\text{-}10\text{-}(\mu\text{-}H)\text{-}10\text{-}endo\text{-}\{Au(PPh_3)\}\text{-}7,8\text{-}R'_2\text{-}nido\text{-}7,8\text{-}C_2B_9H_8]$ (R′ = Me (**2c**), H (**2d**)). The compounds **2** were characterized by microanalysis (see Experimental Section) and by their NMR spectra (Tables I and II). Discussion of the NMR data is deferred, however, until the results of an X-ray diffraction study on **2a** are described.

Selected bond distances and angles are listed in Table III, and the molecular structure is shown in Figure 1. The $Au(PPh_3)$ group is bonded to the *nido*-icosahedral $7,8\text{-}C_2B_9$ fragment primarily through B(4) [Au–B(4) = 2.22(2) Å] with weaker attachments to B(3) and B(5) [Au–B(3) = 2.57(2); Au–B(5) = 2.58(2) Å]. The Ph_3P–Au–B(4) unit is *endo*-related to the C(1)C(2)B(3)B(4)B(5) pentagonal ring with P(3)–Au–B(3) = 143.5(4), P(3)–Au–B(4) = 172.0(5), and P(3)–Au–B(5) = 135.0(4)°. Indeed the structural parameters for the $10\text{-}endo\text{-}\{Au(PPh_3)\}\text{-}7,8\text{-}Me_2\text{-}nido\text{-}7,8\text{-}C_2B_9H_9$ fragment in **2a** are very similar to those found[3] previously for the anion of **1b** [Au–B = 2.486(9), 2.222(9), and 2.528(9) Å; P–Au–B = 143.53(21), 169.29(24), and 138.08(21)°].

The platinum atom is attached to the carborane cage through B(4) *via* an exopolyhedral three-center two-electron B–H→Pt

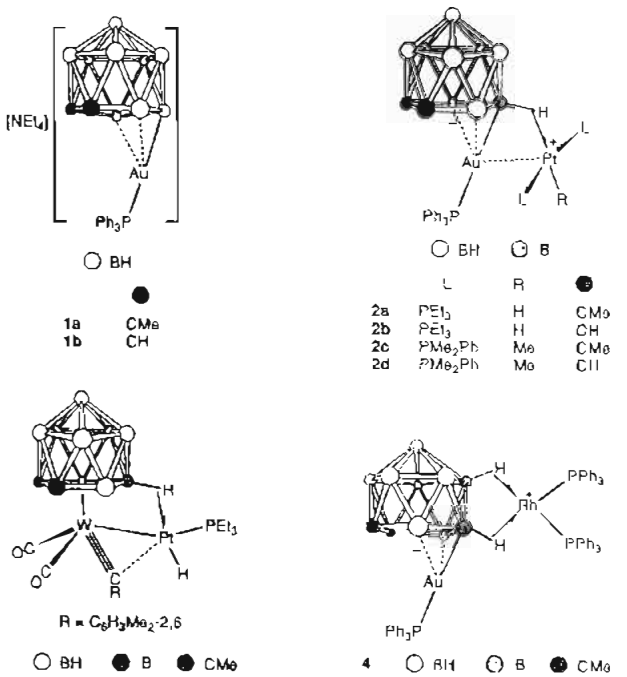

(3) Hamilton, E. J. M.; Welch, A. J. *Polyhedron* **1990**, *9*, 2407.

* To whom correspondence should be addressed.

(1) (a) University of Bristol. (b) Baylor University.

(2) (a) Howard, J. A. K.; Jeffery, J. C.; Jelliss, P. A.; Sommerfeld, T.; Stone, F. G. A. *J. Chem. Soc., Chem. Commun.* **1991**, 1664. (b) Jeffery, J. C.; Jelliss, P. A.; Stone, F. G. A. *J. Chem. Soc., Dalton Trans.* **1993**, 1073. (c) Jeffery, J. C.; Jelliss, P. A.; Stone, F. G. A. *J. Chem. Soc., Dalton Trans.* **1993**, 1083.

0020-1669/93/1332-3943$04.00/0

Table I. ^1H and ^{13}C NMR Data[a] for the Platinum–Gold Complexes

compd	$^1H^b$ (δ)	$^{13}C^c$ (δ)
2a	−12.60 [s, br, 1 H, PtH, *J*(PtH) 1283], −5.72 [q, br, 1 H, BHPt, *J*(BH) *ca.* 60, *J*(PtH) *ca.* 480], 0.94 [d of t, 18 H, CH_2*Me*, *J*(PH) 16, *J*(HH) 9], 1.01 (s, 6H, CMe), 1.86 (m, br, 12 H, CH_2Me), 7.45–7.68 (m, 15 H, Ph)	134.4 [d, C^2(Ph), *J*(PC) 13], 131.1 [C^4(Ph)], 131.0 [d, C^1(Ph), *J*(PC) 51], 128.9 [d, C^3(Ph), *J*(PC) 11], 53.9 (br, *C*Me), 22.6 (C*Me*), 18.7 [(AXX′), *C*H_2Me, *N* 34,[d] *J*(PtC) 42], 8.4 [CH_2*Me*, *J*(PtC) 29]
2b	−12.74 [s, br, 1 H, PtH, *J*(PtH) 1276], −5.79 [q, br, 1 H, BHPt, *J*(BH) *ca.* 70, *J*(PtH) *ca.* 460], 0.91 [d of t, 18 H, CH_2*Me*, *J*(PH) 16, *J*(HH) 8], 1.52 (s, br, 2 H, CH), 1.84 (m, br, 12 H, CH_2Me), 7.44–7.68 (m, 15 H, Ph)	134.7 [d, C^2(Ph), *J*(PC) 13], 132.1 [d, C^1(Ph), *J*(PC) 53], 131.5 [C^4(Ph)], 129.3 [d, C^3(Ph), *J*(PC) 11], 39.6 (br, CH), 19.1 [(AXX′), *C*H_2Me, *N* 33,[d] *J*(PtC) 44], 8.6 [CH_2*Me*, *J*(PtC) 28]
2e	−6.34 [q, br, 1 H, BHPt, *J*(BH) *ca.* 60, *J*(PtH) *ca.* 430], −0.15 [t, 3 H, MePt, *J*(PH) 8, *J*(PtH) 74], 1.04 (s, 6 H, CMe), 1.80 [(AXX′), 6 H, MeP, *N* 7,[d] *J*(PtH) *ca.* 30], 1.84 [(AXX′), 6 H, MeP, *N* 8,[d] *J*(PtH) *ca.* 26], 7.13–7.56 (m, 25 H, Ph)	[e] 134.4–127.9 (Ph), 22.7 (C*Me*), 15.4 [(AXX′), MeP, *N* 37[d]], 12.6 [(AXX′), MeP, *N* 35[d]], −1.6 [t, MePt, *J*(PC) 8]
2d	−6.34 [q, br, 1 H, BHPt, *J*(BH) *ca.* 60, *J*(PtH) *ca.* 400], −0.18 [t, 3 H, MePt, *J*(PH) 9, *J*(PtH) 73], 1.58 (s, br 2 H, CH), 1.77 [(AXX′), 6 H, MeP, *N* 7,[d] *J*(PtH) *ca.* 32], 1.79 [(AXX′), 6 H, MeP, *N* 7,[d] *J*(PtH) *ca.* 24], 7.06–7.57 (m, 25 H, Ph)	[e] 134.5–128.3 (Ph), 39.1 (br, CH), 15.9 [(AXX′), MeP, *N* 38[d]], 13.3 [(AXX′), MeP, *N* 37[d]], −2.6 [t, MePt, *J*(PC) 9]

[a] Chemical shifts δ in ppm, coupling constants *J* in Hz. Measurements at ambient temperatures and in CD_2Cl_2 unless otherwise stated. [b] Resonances for terminal BH protons occur as broad unresolved weak signals in the range δ *ca.* −2 to 3. [c] Hydrogen-1 decoupled, chemical shifts are positive to high frequency of $SiMe_4$ (0.0 ppm). [d] Insufficient resolution prevents full analysis of coupling constants; $N = |J(AX) + J(AX')|$. [e] Measured in CD_2Cl_2–THF (4:1). Compound decomposes in solution, and its relative insolubility results in the non-observation of ^{195}Pt satellite peaks and resonance due to cage *C*Me nuclei in **2c**.

Table II. ^{11}B and ^{31}P NMR Data[a] for the Platinum–Gold Complexes

compd	$^{11}B^b$ (δ)	$^{31}P^c$ (δ)
2a	−9.4 (1 B), −15.4 (2 B), −18.4 (2 B), −19.7 (2 B), −30.8* (1 B), −37.1 (1 B)	37.4 (m, br, 1 P, PAu), 16.9 [s, 2 P, PPt, *J*(PtP) 2640]
2b	−17.6 (5 B), −24.0 (2 B), −29.5* (1 B), −38.0 (1 B)	36.6 (m, br, 1 P, PAu), 17.0 [s, 2 P, PPt, *J*(PtP) 2663]
2c	−7.3 (1 B), −13.5 (2 B), −16.5 (2 B), −18.0 (2 B), −26.7* (1 B), −35.7 (1 B)	39.8 (m, br, 1 P, PAu), −5.4 [s, 2 P, PPt, *J*(PtP) 2825]
2d	−17.6 (5 B), −23.8 (2 B), −27.1* (1 B), −38.4 (1 B)	37.8 (m, br, 1 P, PAu), −6.4 [s, 2 P, PPt, *J*(PtP) 2843]

[a] Chemical shifts δ in ppm, coupling constants *J* in Hz. Measurements at ambient temperatures in CD_2Cl_2. [b] Hydrogen-1 decoupled, measurements at 128.3 MHz, chemical shifts are positive to high frequency of BF_3·Et_2O (external). All resonances are broad, with some signals corresponding to overlapping peaks which do not necessarily indicate symmetry equivalence. Peaks marked with an asterisk are ascribed to the B–H→Pt groups, becoming very broad in ^1H-coupled spectra due to unresolved ^1H–^{11}B coupling (*ca.* 60–70 Hz, see Table I). Other resonances in ^{11}B spectra are doublets with $J(HB) > 100$ Hz. [c] Hydrogen-1 decoupled, measurements at 161.9 MHz, chemical shifts are positive to high frequency of 85% H_3PO_4 (external).

bond. Although H(4) was not located in the electron-density difference map, nevertheless, its position is in accord with that calculated using the steric-potential-energy-minimization technique.[4] This also applies to the terminal hydride H(01), and both H(01) and H(4) were unambiguously revealed by ^1H NMR spectroscopy, as discussed below. The two PEt_3 ligands are transoid to one another [P(1)–Pt–P(2) = 163.6(2)°; P–Pt average 2.298 Å], and hence the platinum is in a distorted square planar environment since H(01) and B(4)–H(4) are also transoid to one another. A similar arrangement of terminal Pt–H and bridging B–H→Pt bonds occurs in the complex [WPtH(μ-$CC_6H_3Me_2$-2,6)(CO)$_2$(PEt_3)(η^5-7,8-Me_2-7,8-$C_2B_9H_9$)] (**3**).[5] Formally, the B(4)–H(4) bond in **2a** donates an electron pair to stabilize the $[PtH(PEt_3)_2]^+$ cation. Overall the molecule may be regarded as being zwitterionic in character, with a cationic $[PtH(PEt_3)_2]^+$ fragment linked to the anion [10-*endo*-{Au(PPh_3)}-7,8-Me_2-*nido*-7,8-$C_2B_9H_9$]$^-$ by the three-center B(4)–H(4)→Pt bond. This view of the bonding, however, may be too simplistic because it neglects any direct Au–Pt interaction.

In several gold–platinum cluster compounds Au–Pt separations have been generally observed in the range 2.590–2.843 Å,[6] and as expected the shorter distances are found in cationic polynuclear species and the longer in neutral clusters. The Au–Pt separation in **2a** [3.000(1) Å] is long and is probably influenced by the steric and electronic requirements of the bridging carborane cage. However, some direct metal–metal bonding is probable. Relevant to the present study are the dimetal gold–platinum salts [PtAu(C_6F_5)(μ-H)(PEt_3)$_2$(PPh_3)][SO_3CF_3] [Au–Pt = 2.714(1) Å][7a] and [PtAu(C_6Cl_5)(μ-H)(PPh_3)$_3$][ClO_4] [Au–Pt = 2.792(1) Å].[7b] In the anions of these salts an essentially square-planar *trans*-Pt(H)(X)(PR_3)$_2$ (X = C_6F_5 or C_6Cl_5, R = Et or Ph) unit and an almost linear $HAu(PPh_3)$ fragment share a bridging hydrido ligand. In **2a** the carborane cage functions as the bridge [Au–B(4)–Pt = 75.8(5)°] between a nearly linear P(3)–Au–B(4) [172.0(5)°] group and a platinmum atom in a distorted square-planar environment. Direct metal–metal bonding in the cations $[PtAuX(\mu\text{-}H)(PR_3)_2(PPh_3)]^+$ has been described in terms of donation of an electron pair from a d-orbital of platinum into a vacant p-orbital on the gold (Figure 3A).[7a] A similar interaction between the gold and the platinum atoms is suggested for complexes of type **2** (Figure 3B), with the d_{xz} or possibly the d_{z^2} acting as the donor orbital (simple angular calculations were indeterminate). The relatively long Au–Pt separation in **2a**, indicative of weak metal–metal bonding, may be due to a combination of the effects of the bulky PPh_3 and PEt_3 groups keeping the two metal atoms apart and to nonalignment of the bonding orbitals in the metal–metal bond leading to their poor overlap. The relatively high energy of the gold p-orbital relative to the platinum d-orbital may also contribute to weak metal–metal bonding.

The usual "slip" and "fold" distortions of the metallacarborane cage[8] are observed in the structure of **2a**, and these are Δ = 1.00 Å, φ = 2.6°, and θ = 1.1°. For the anion [10-*endo*-{Au(PPh_3)}-*nido*-7,8-$C_2B_9H_{11}$]$^-$ the corresponding data are Δ = 0.87 Å, ϕ = 3.28°, and θ = 3.15°.[3] The greater slippage of the gold atom toward the β-boron atom in **2a** compared with the anion of **1b** is as expected with the Au–Pt bonding. However, for the molecule [5,10-*exo*-{Rh(PPh_3)$_2$}-5,10-(μ-H)$_2$-10-*endo*-{Au(PPh_3)}-7,8-Me_2-*nido*-7,8-$C_2B_9H_7$] (**4**)[2b] (Δ = 1.05 Å, ϕ = 6.1°, and θ

(4) Orpen, A. G. *J. Chem. Soc., Dalton Trans.* **1980**, 2509.
(5) Devore, D. D.; Howard, J. A. K.; Jeffery, J. C.; Pilotti, M. U.; Stone, F. G. A. *J. Chem. Soc., Dalton Trans.* **1989**, 303.
(6) (a) Payne, N. C.; Ramachandran, R.; Schoettel, G.; Vittal, J. J.; Puddephatt, R. J. *Inorg. Chem.* **1991**, *30*, 4048. (b) Ito, L. N.; Felicissimo, A. M. P.; Pignolet, L. H. *Inorg. Chem.* **1991**, *30*, 387. (c) Mingos, D. M. P.; Oster, P.; Sherman, D. J. *J. Organomet. Chem.* **1987**, *320*, 257.
(7) (a) Albinati, A.; Lehner, L.; Venanzi, L. M.; Wolfer, M. *Inorg. Chem.* **1987**, *26*, 3933. (b) Crespo, M.; Sales, J.; Solans, X. *J. Chem. Soc., Dalton Trans.* **1989**, 1089.
(8) Forsyth, M. I.; Mingos, D. M. P.; Welch, A. J. *J. Chem. Soc., Dalton Trans.* **1978**, 1363.

Table III. Selected Internuclear Distances (Å) and Angles (deg) for the Complex [10-*exo*-{Pt(H)(PEt_3)$_2$}-10-(μ-H)-10-*endo*-{Au(PPh_3)}-7,8-Me_2-*nido*-7,8-$C_2B_9H_8$] (**2a**)

Au···Pt	3.000(1)	Au–P(3)	2.274(4)	Au–B(3)	2.57(2)	Au–B(4)	2.22(2)
Au–B(5)	2.58(2)	Pt–H(01)	1.65[a]	Pt–P(1)	2.300(4)	Pt–P(2)	2.296(5)
Pt–B(4)	2.63(2)	Pt–H(4)	1.76[a]	C(1)–C(2)	1.58(2)	C(1)–B(5)	1.58(3)
C(1)–B(6)	1.76(3)	C(1)–B(10)	1.71(3)	C(1)–C(10)	1.54(3)	C(2)–B(3)	1.63(2)
C(2)–B(6)	1.72(3)	C(2)–B(7)	1.72(3)	C(2)–C(20)	1.49(3)	B(3)–B(4)	1.84(3)
B(3)–B(7)	1.80(3)	B(3)–B(8)	1.78(3)	B(4)–B(5)	1.81(2)	B(4)–B(8)	1.79(3)
B(4)–B(9)	1.75(3)	B(4)–H(4)	1.34[a]	B(5)–B(9)	1.75(3)	B(5)–B(10)	1.75(3)
B(6)–B(7)	1.73(3)	B(6)–B(10)	1.73(3)	B(6)–B(11)	1.70(3)	B(7)–B(8)	1.74(3)
B(7)–B(11)	1.76(3)	B(8)–B(9)	1.78(3)	B(8)–B(11)	1.77(3)	B(9)–B(10)	1.76(3)
B(9)–B(11)	1.80(3)	B(10)–B(11)	1.77(3)				

Pt–Au–P(3)	116.1(1)	Pt–Au–B(3)	88.1(4)	P(3)–Au–B(3)	143.5(4)
Pt–Au–B(4)	58.3(4)	P(3)–Au–B(4)	172.0(5)	B(3)–Au–B(4)	44.4(6)
Pt–Au–B(5)	90.2(4)	P(3)–Au–B(5)	135.0(4)	B(3)–Au–B(5)	66.3(6)
B(4)–Au–B(5)	43.6(6)	Au–Pt–H(01)	118[a]	Au–Pt–P(1)	93.8(1)
H(01)–Pt–P(1)	87[a]	Au–Pt–P(2)	101.8(1)	H(01)–Pt–P(2)	82[a]
P(1)–Pt–P(2)	163.6(2)	Au–Pt–B(4)	45.9(4)	H(01)–Pt–B(4)	164[a]
P(1)–Pt–B(4)	96.8(4)	P(2)–Pt–B(4)	97.8(4)	Au–Pt–H(4)	73[a]
H(01)–Pt–H(4)	169[a]	P(1)–Pt–H(4)	95[a]	P(2)–Pt–H(4)	95[a]
B(4)–Pt–H(4)	27[a]	Pt–P(1)–C(31)	112.3(6)	Pt–P(1)–C(33)	114.5(7)
C(31)–P(1)–C(33)	104(1)	Pt–P(1)–C(35)	114.7(7)	C(31)–P(1)–C(35)	107(1)
C(33)–P(1)–C(35)	103.4(9)	Pt–P(2)–C(41)	113.2(7)	Pt–P(2)–C(43)	110.5(7)
C(41)–P(2)–C(43)	105(1)	Pt–P(2)–C(45)	119(1)	C(41)–P(2)–C(45)	102(1)
C(43)–P(2)–C(45)	105(1)	Au–P(3)–C(51)	115.6(5)	Au–P(3)–C(61)	114.8(5)
C(51)–P(3)–C(61)	105.3(7)	Au–P(3)–C(71)	112.8(5)	C(51)–P(3)–C(71)	104.1(7)
C(61)–P(3)–C(71)	102.9(7)	Au–B(3)–C(2)	90.4(9)	Au–B(3)–B(4)	57.7(7)
Au–B(3)–B(7)	144(1)	Au–B(3)–B(8)	117(1)	Au–B(3)–H(3)	92[a]
Au–B(4)–Pt	75.8(5)	Au–B(4)–B(3)	77.9(8)	Pt–B(4)–B(3)	120(1)
Au–B(4)–B(5)	78.7(8)	Pt–B(4)–B(5)	125(1)	Au–B(4)–B(8)	136(1)
Pt–B(4)–B(8)	127(1)	Au–B(4)–B(9)	138(1)	Pt–B(4)–B(9)	130(1)
Au–B(4)–H(4)	113[a]	Pt–B(4)–H(4)	37[a]	B(3)–B(4)–H(4)	129[a]
B(5)–B(4)–H(4)	130[a]	B(8)–B(4)–H(4)	99[a]	B(9)–B(4)–H(4)	98[a]
Au–B(5)–C(1)	89(1)	Au–B(5)–B(4)	57.7(7)	Au–B(5)–B(9)	116(1)
Au–B(5)–B(10)	144(1)	Au–B(5)–H(5)	92[a]		

[a] H(01) and H(4) in calculated positions (see Experimental Section).

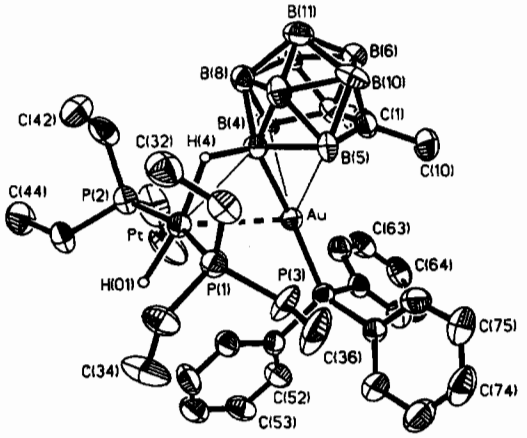

Figure 1. Structure of [10-*exo*-{Pt(H)(PEt_3)$_2$}-10-(μ-H)-10-*endo*-{Au(PPh_3)}-7,8-Me_2-*nido*-7,8-$C_2B_9H_8$] (**2a**). Thermal ellipsoids are shown at 40% probability level.

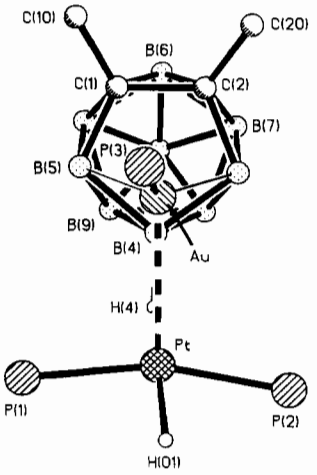

Figure 2. View of complex **2a** demonstrating that a non-crystallographic molecular symmetry plane passes through the atoms H(01), Pt, B(4), Au, and P(3) and the midpoint of the C(1)–C(2) connectivity. The Et and Ph groups are omitted for clarity.

= 2.2°) the gold atom slippage is greater, surprisingly so as there is no metal–metal bond in the gold–rhodium species.

Having established the structure of compound **2a**, the NMR data are readily interpreted, as are those of **2b–2d**, because similarities in the spectra indicate that the structures of all the complexes are alike. In the ^{1}H NMR spectrum of **2a** the presence of the terminally bound hydrido ligand on the platinum is unambiguously shown by the resonance at δ −12.60 with ^{195}Pt–^{1}H satellite peaks [J(PtH) = 1283 Hz].[9] A diagnostic quartet signal[10] for the B–H→Pt group is observed at δ −5.72 [J(BH) ≃ 60, J(PtH) ≃ 480 Hz], the individual peaks being broad. These data may be compared with those obtained from the ^{1}H NMR spectra of compound **3** [δ −10.22, PtH, J(PtH) = 1165 Hz, and δ −4.7, br, B–H→Pt].[5] The structure of **2a** shows (Figure 2) that the atoms H(01), Pt, Au, B(4), and P(3), and the midpoint of the C(1)–C(2) vector lie on a molecular symmetry plane. Consequently, the carborane cage CMe groups are chemically equivalent, giving rise to one resonance in the ^{1}H NMR spectrum (δ 1.01) and two in the ^{13}C{^{1}H} NMR spectrum [δ 53.9 (*C*Me) and 22.6 (C*Me*)]. The symmetry of the molecule also leads to the observation of one signal [δ 16.9, J(PtP) = 2640 Hz] in the ^{31}P{^{1}H} NMR spectrum for the two PEt_3 groups, these ligands lying on either side of the symmetry plane. The resonance for the Au(PPh_3) group appears as a broad multiplet at δ 37.4. The signal for this moiety in the ^{31}P{^{1}H} NMR spectrum of **1a** is at δ 40.5, and is also broad. The broadness of the peaks may be attributed to unresolved coupling with the transoid boron nuclei.

(9) Roundhill, D. M.; *Adv. Organomet. Chem.*, **1975**, *13*, 273. Kaesz, H. D.; Saillant, R. B. *Chem. Rev.* **1972**, *72*, 231.
(10) Brew, S. A.; Stone, F. G. A. *Adv. Organomet. Chem.* **1993**, *35*, 135.

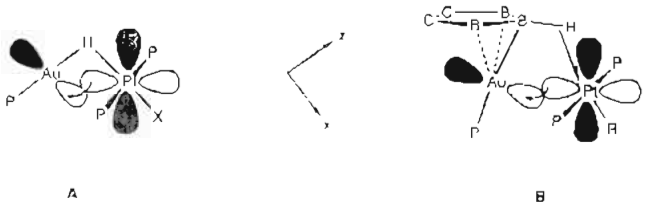

Figure 3. Qualitative representation of the direct Au–Pt bonding: (A) in the cations $[PtAu(X)(\mu\text{-}H)(PR_3)_3]^+$ [7a] and (B) in the complexes **2**. Only the atoms in the open pentagonal face of the *nido*-7,8-C_2B_9 cage are shown.

The ^1H NMR spectra (Table I) of the compounds **2b–2d** all display diagnostic quartet signals for their B–H→Pt groups, with $^{195}Pt–^1H$ couplings as expected in the 400–460-Hz range.[5,11] The terminal PtH group in **2b** resonates at δ –12.74 [J(PtH) = 1276 Hz], while the PtMe groups in **2c** and **2d** give rise to triplet peaks at δ –0.15 and –0.18, with J(PH) = 8 and 9 Hz, and with J(PtH) = 74 and 73 Hz, respectively. The $^{31}P\{^1H\}$ NMR spectra (Table II) of **2b–2d** were as expected, each spectrum showing two resonances, one broad band for the $Au(PPh_3)$ group and a singlet of approximately twice the intensity for the two equivalent phosphine ligands of the transoid $Pt(PR_3)_2$ groups.

The $^{11}B\{^1H\}$ NMR spectrum of **2a** (Table II) displays six broad overlapping peaks for the nine boron atoms. A fully coupled ^{11}B spectrum was measured to assign the resonance due to the B–H→Pt group. This experiment resulted in all but one of the peaks becoming doublets with J(BH) > 100 Hz. The resonance at δ –30.8, corresponding in intensity to one boron nucleus, became very broad due to unresolved $^1H–^{11}B$ coupling (*ca.* 60 Hz, Table I), and is assigned to B(4) (Figure 1). Similarly, examination of the proton-coupled ^{11}B spectra of compounds **2b–2d** revealed in each spectrum (Table II) one peak due to a single boron atom which occurred as a broad unresolved resonance. The ^{11}B chemical shifts observed for the *B*–H→Pt nuclei (δ –26.7 to –30.8) are outside the range (δ *ca.* 10–30) normally found for dimetal complexes containing exopolyhedral B–H→metal groups when the boron atom is part of a *closo*-icosahedral metallacarborane structure.[10] However, the complexes **2** contain *nido*- and not *closo*-icosahedral cages, and in this respect are more closely related to the zwitterionic species [9,10-*exo*-{$W(CO)_2(\eta^5\text{-}C_5R_5)$}-9,10-($\mu$-H)$_2$-10,11-*endo*-($\mu$-H)-7,8-$Me_2$-*nido*-$C_2B_9H_7$] (R = H or Me).[12] The [^{11}B-^{11}B]-COSY NMR spectra of these tungsten compounds revealed that the *B*–H→W nuclei give rise to relatively shielded signals at δ *ca.* –50.

It is apparent that the complexes **2** do not display dynamic behavior on the NMR time scale at room temperature, in contrast with compound **4**[2b] and the species [*exo*-{$Rh(PPh_3)_2$}-7,8-Me_2-*nido*-7,8-$C_2B_9H_{10}$],[13] isolobally related to **4**. In the rhodium complexes the $Rh(PPh_3)_2$ fragment rotates and migrates about the polyhedral surface of the cage. Consequently, in fully coupled ^{11}B spectra no boron resonances with J(BH) values less than 100 Hz are observed. In the compounds **2** cleavage of the Au–Pt bond could allow the $Pt(R)L_2$ groups to rotate, and to switch to linking with the B–H bonds α to the carbon atoms in the face of the cage.[5,14] However, measurements of the ^1H and $^{31}P\{^1H\}$ NMR spectra of **2a** down to –90 °C revealed no change, as might be expected if dynamic behavior involving rapid equilibration between B_β–H→Pt and B_α–H→Pt bonding modes were to be frozen out. Most important in this context is the above mentioned observation in room temperature proton-coupled ^{11}B spectra of the broad unresolved signal corresponding to one boron nucleus. This implies that the $Pt(R)L_2$ fragment is only associated with the β-boron atom in the face of carborane cage and does not interchange. The B_β–H→Pt linkages in the complexes **2** are thus probably supported by the Au–Pt bonding.

Conclusions

The results described in this paper, together with those reported earlier,[2] illustrate the potential of the salts **1** in the synthesis of metallacarborane compounds with unusual structures. Although numerous di- and polynuclear metal compounds containing gold and platinum are known,[15] the complexes **2** are structurally without precedent.

Experimental Section

Reagents and Instrumentation. All solvents were freshly distilled under nitrogen from appropriate drying agents before use. Chromatography columns, *ca.* 15 cm long and 3 cm in diameter, were packed with silica (70–100 mesh). Columns were maintained at *ca.* –30 °C for isolation of product. All experiments were conducted under nitrogen using Schlenk tube techniques. The NMR measurements were made using a JEOL JNM 400-MHz spectrometer. The reagents [NEt_4][10-*endo*-{$Au(PPh_3)$}-7,8-Me_2-*nido*-7,8-$C_2B_9H_9$] (**1a**),[2b] [$PtCl(H)(PEt_3)_2$],[16] and [$PtCl(Me)(PMe_2Ph)_2$][17] were prepared as described previously. The salt **1b** was obtained using the procedure employed to obtain its [$N(CH_2Ph)Me_3$]$^+$ analog.[3]

Synthesis of the Platinum–Gold Compounds. (i) A mixture of the compounds **1a** (0.22 g, 0.29 mmol) and [$PtCl(H)(PEt_3)_2$] (0.14 g, 0.29 mmol) in CH_2Cl_2 (20 mL) was stirred for *ca.* 12 h. After the solvent had been reduced in volume *in vacuo* to about 2 mL, the remaining material was chromatographed. Elution initially with CH_2Cl_2–*n*-hexane (1:1), followed by neat CH_2Cl_2, afforded a broad yellow band. After removal of solvent *in vacuo*, the residue was crystallized from CH_2Cl_2–*n*-hexane (10 mL, 1:4) to give, after drying *in vacuo*, orange microcrystals of [10-*exo*-{$Pt(H)(PEt_3)_2$}-10-(μ-H)-10-*endo*-{$Au(PPh_3)$}-7,8-Me_2-*nido*-7,8-$C_2B_9H_8$] (**2a**) (0.13 g, 59%). Anal. Calcd for $C_{34}H_{61}AuB_9P_3Pt$: C, 38.8; H, 5.8. Found: C, 39.2; H, 6.1.

(ii) In a similar manner, the compounds **1b** (0.13 g, 0.18 mmol) and [$PtCl(H)(PEt_3)_2$] (0.08 g, 0.18 mmol) in CH_2Cl_2 (15 mL) were stirred together for *ca.* 12 h. After the solvent had been reduced in volume to *ca.* 2 mL, the mixture was chromatographed. Elution initially with CH_2Cl_2–*n*-hexane (2:3), followed by neat CH_2Cl_2, afforded a yellow fraction. After removal of solvent *in vacuo*, the residue was crystallized from CH_2Cl_2–*n*-hexane (10 mL, 1:4) to afford orange microcrystals of [10-*exo*-{$Pt(H)(PEt_3)_2$}-10-(μ-H)-10-*endo*-{$Au(PPh_3)$}-*nido*-7,8-$C_2B_9H_{10}$] (**2b**) (0.09 g, 66%). Anal. Calcd for $C_{32}H_{57}AuB_9P_3Pt$: C, 37.5; H, 5.6. Found: C, 38.2; H, 6.2.

(iii) Treatment of the salt **1a** (0.15 g, 0.20 mmol) with [$PtCl(Me)(PMe_2Ph)_2$] (0.10 g, 0.20 mmol) in CH_2Cl_2 (20 mL) for 12 h, followed by an isolation procedure similar to that described above, gave orange microcrystals of [10-*exo*-{$Pt(Me)(PMe_2Ph)_2$}-10-(μ-H)-10-*endo*-{$Au(PPh_3)$}-7,8-Me_2-*nido*-7,8-$C_2B_9H_8$] (**2c**) (0.11 g, 63%). Anal. Calcd for $C_{39}H_{55}AuB_9P_3Pt$: C, 42.3; H, 5.0. Found: C, 42.3; H, 5.4.

(iv) Following the method used to obtain **2a**, the compound [10-*exo*-{$Pt(Me)(PMe_2Ph)_2$}-10-(μ-H)-10-*endo*-{$Au(PPh_3)$}-*nido*-7,8-$C_2B_9H_{10}$] (**2d**) (0.15 g, 48%) was isolated from the reagent **1b** (0.23 g, 0.32 mmol) and [$PtCl(Me)(PMe_2Ph)_2$] (0.17 g, 0.32 mmol). Orange crystals were obtained by crystallization from CH_2Cl_2–*n*-*hexane* (10 mL, 1:3) and drying *in vacuo*. Anal. Calcd for $C_{37}H_{51}AuB_9P_3Pt$: C, 41.2; H, 4.8. Found: C, 39.9; H, 5.0.

Crystallography. Orange prismatic crystals of **2a** were grown by diffusion of *n*-hexane into a CH_2Cl_2 solution of the compound. The crystal used for data collection (dimensions 0.13 × 0.23 × 0.43 mm) was

(11) Attfield, M. J.; Howard, J. A. K.; Jelfs, A. N. de M.; Nunn, C. M.; Stone, F. G. A. *J. Chem. Soc., Dalton Trans.* **1987**, 2219. Goldberg, J. E.; Mullica, D. F.; Sappenfield, E. L.; Stone, F. G. A. *J. Chem. Soc., Dalton Trans.* **1993**, 281.
(12) Brew, S. A.; Jeffery, J. C.; Mortimer, M. D.; Stone, F. G. A. *J. Chem. Soc., Dalton Trans.* **1992**, 1365.
(13) Long, J. A.; Marder, T. B.; Behnken, P. E.; Hawthorne, M. F. *J. Am. Chem. Soc.* **1984**, *106*, 2979; Hawthorne, M. F. Chapter 10 In *Advances in Boron and the Boranes*; Eds. Liebman, J. F., Greenberg, A., Williams, R. E., Eds.; VCH Publishers Inc.: New York, 1988.
(14) Jeffery, J. C.; Ruiz, M. A.; Stone, F. G. A. *J. Chem. Soc., Dalton Trans.* **1989**, 1845.
(15) (a) Hall, K. P.; Mingos, D. M. P. *Prog. Inorg. Chem.* **1984**, *32*, 237. (b) Salter, I. D. *Adv. Organomet. Chem.* **1989**, *29*, 249.
(16) Parshall, G. W. *Inorg. Synth.* **1970**, *12*, 28.
(17) Carr, N.; Gimeno, M. C.; Stone, F. G. A. *J. Chem. Soc., Dalton Trans.* **1990**, 2617.

Table IV. Crystallographic Data[a] for **2a**

molecular formula	$C_{34}H_{61}AuB_9P_3Pt$	μ(Mo Kα)/cm^{-1}	68.9
fw	1052.1	T/K	293
cryst syst	monoclinic	data collcn limits (2θ), deg	5–55
space group	*Cc*	no. of data collcd (excl. stds)	5226
a, Å	11.092(3)	no. of unique data	5076
b, Å	20.235(7)	no. of obsd data used	4376
c, Å	18.998(6)	criterion for data (n) used [$F_o \geq n\sigma(F_o)$]	4
β, deg	96.10(3)	no. of params refined	440
V, Å^3	4240(2)	R (R_w)[b]	0.048 (0.049)
Z	4	goodness-of-fit	1.06
d_{calc}, g/cm^3	1.65	final electron density diff features (max; min), e Å^{-3}	2.80; −2.04
F(000)	2048		

[a] Data collected on a Siemens R3m/V four-circle diffractometer operating in the Wyckoff ω-scan mode; graphite-monochromated Mo Kα X-radiation, λ = 0.710 73 Å. Refinement was by full-matrix least-squares with a weighting scheme of the form $w^{-1} = [\sigma^2(F_o) + 0.0015|F_o|^2]$; $\sigma^2(F_o)$ is the variance in F_o due to counting statistics; g was chosen so as to minimize variation in $\sum w(|F_o| - |F_c|)^2$ with $|F_o|$. [b] $R = \sum||F_o| - |F_c||/\sum|F_o|$; $R_w = \sum w^{1/2}||F_o| - |F_c||/\sum w^{1/2}|F_o|$.

Table V. Atomic Positional Parameters (Fractional Coordinates × 10^4) and Equivalent Isotropic Thermal Parameters U_{eq} (Å^2 × 10^3) for Compound **2a**, with Estimated Standard Deviations in Parentheses

atom	x	y	z	U_{eq}[a]
Au[b]	0	1004(1)	0	42(1)
Pt	2696(1)	1158(1)	298(1)	45(1)
P(1)	2850(4)	1819(2)	−673(2)	48(1)
P(2)	3126(4)	465(2)	1248(3)	53(1)
P(3)	−656(4)	276(2)	−869(2)	43(1)
C(1)	−1563(15)	2103(9)	453(9)	53(5)
C(2)	−1541(14)	1596(7)	1083(9)	46(5)
B(3)	−172(15)	1315(10)	1299(9)	46(5)
B(4)	823(15)	1765(9)	747(10)	43(5)
B(5)	−279(16)	2253(9)	199(11)	50(6)
B(6)	−1744(21)	2409(11)	1305(12)	60(7)
B(7)	−813(17)	1905(11)	1860(11)	55(6)
B(8)	650(17)	2021(10)	1631(10)	49(6)
B(9)	606(16)	2601(9)	924(11)	52(6)
B(10)	−920(21)	2838(10)	728(12)	60(7)
B(11)	−358(21)	2702(11)	1623(12)	61(7)
C(10)	−2702(17)	2123(13)	−86(12)	77(8)
C(20)	−2558(18)	1126(10)	1138(15)	80(9)
C(31)	2905(18)	2694(8)	−447(10)	59(6)
C(32)	3888(22)	2863(10)	130(13)	78(8)
C(33)	4246(20)	1691(11)	−1110(11)	71(7)
C(34)	4467(29)	1026(12)	−1375(17)	105(12)
C(35)	1641(18)	1708(13)	−1392(9)	72(8)
C(36)	1699(23)	2170(17)	−2024(12)	109(12)
C(41)	3307(22)	897(12)	2092(10)	78(8)
C(42)	4140(26)	1470(15)	2114(14)	93(11)
C(43)	4570(16)	37(10)	1189(11)	63(6)
C(44)	5165(24)	−283(12)	1827(13)	88(9)
C(45)	2060(24)	−183(12)	1407(20)	105(13)
C(46A)	1767(38)	−637(17)	956(24)	116(19)
C(46B)	2166(76)	−614(50)	1885(35)	79(34)
C(51)	421(15)	−361(8)	−1051(9)	46(5)
C(52)	117(19)	−988(9)	−1281(11)	63(6)
C(53)	968(22)	−1451(10)	−1407(12)	73(8)
C(54)	2195(21)	−1302(11)	−1243(11)	73(8)
C(55)	2488(17)	−676(10)	−1024(12)	73(8)
C(56)	1638(15)	−218(9)	−894(10)	57(6)
C(61)	−2061(13)	−171(8)	−725(9)	44(5)
C(62)	−2202(15)	−331(8)	−23(9)	54(5)
C(63)	−3216(20)	−697(10)	92(12)	68(7)
C(64)	−4056(16)	−889(10)	−435(13)	70(7)
C(65)	−3888(17)	−714(11)	−1108(12)	71(7)
C(66)	−2915(17)	−359(9)	−1257(11)	61(6)
C(71)	−1050(14)	675(8)	−1726(8)	43(5)
C(72)	−753(19)	402(11)	−2351(10)	68(7)
C(73)	−1121(23)	715(15)	−2996(12)	89(10)
C(74)	−1694(22)	1325(14)	−2998(13)	87(9)
C(75)	−2024(22)	1588(12)	−2367(12)	83(9)
C(76)	−1663(22)	1267(10)	−1740(11)	68(7)

[a] Equivalent isotropic U_{eq} defined as one-third of the trace of the orthogonalized U_{ij} tensor. [b] Polar space group requires first metal atom in list to have x and z coordinates fixed.

cut from a larger crystal and was mounted in a sealed glass capillary under nitrogen. The cell parameters were determined by a least-squares fit of 35 reflections in the range of $15 \leq 2\theta \leq 28°$ located in a random search of the reciprocal lattice. Data collection and reduction information are given in Table IV. Three standard reflections were measured every 97 reflections during data collection and these showed no significant decay. The data were corrected for Lorentz and polarization effects and an empirical absorption correction[18] based on a series of ψ-scans was also applied. The structure was solved by conventional heavy atom methods and successive difference Fourier syntheses were used to locate all non-hydrogen atoms.

All non-hydrogen atoms were refined with anisotropic thermal parameters. Methyl, methylene and phenyl hydrogen atoms were included in calculated positions (C–H = 0.96 Å) with fixed isotropic thermal parameters (U_{iso} = 0.08 Å^2). Terminal cage B–H hydrogen atoms were also included in calculated positions [B–H = 1.1 Å; U_{iso} = 1.2 U_{iso}(B)].[19] The positions of the Pt–H(01) and B(4)–H(4)—Pt hydrogen atoms were determined from steric-potential-energy-minimization calculations[4] and these atoms were included in fixed positions (U_{iso} = 0.08 Å^2) during subsequent refinements. The methyl group bound to carbon atom C(45) in one of the PEt_3 groups was found to occupy two possible positions, C(46A) and C(46B), and these were refined with fixed site occupancy factors of 0.75 and 0.25 respectively, in order to maintain reasonable equivalent isotropic thermal parameters. The calculated hydrogen atoms assigned to C(46A) and C(46B) were given the same fixed site occupancy factors as their parent carbon atoms. As a result of this disorder, there was no assignment of hydrogen atoms to the methylene carbon atom C(45).

The large difference map features in the final difference Fourier synthesis were located close to the metal atoms and can be attributed to the probable presence of a subcrystal, as evidenced by the peak profiles of certain very strong reflections having small side-peaks. The applied absorption correction was satisfactory and unlikely to be the cause of the large residual peaks. All computations were performed on a DEC μ-Vax II computer with the SHELXTL system of programs.[18] Scattering factors with corrections for anomalous dispersion were taken from ref 20 and atomic parameters (x, y, z, U_{eq}'s) are listed in Table V.

Acknowledgment. We thank the U.K. Science and Engineering Research Council for the award of a research studentship (to P.A.J.), and the Robert A. Welch Foundation for support (Grant AA-1201).

Supplementary Material Available: Complete tables of bond lengths and angles, anisotropic thermal parameters, and hydrogen atom parameters for **2a** (11 pages). Ordering information is given on any current masthead page.

(18) Sheldrick, G. M. SHELXTL-PC programs for use with the Siemens X-ray system. Siemens, Madison, WI.
(19) Sherwood, P. BHGEN, a program for the calculation of idealized H-atom positions for a *nido*-icosahedral carborane cage. University of Bristol, 1986.
(20) *International Tables for X-ray Crystallography*; Kynoch Press: Birmingham, England, 1974; Vol. IV.